



## UvA-DARE (Digital Academic Repository)

### Activity- and pharmacology-dependent modulation of adult neurogenesis in relation to Alzheimer's disease

Marlatt, M.W.

**Publication date**  
2012

[Link to publication](#)

#### **Citation for published version (APA):**

Marlatt, M. W. (2012). *Activity- and pharmacology-dependent modulation of adult neurogenesis in relation to Alzheimer's disease*. [Thesis, fully internal, Universiteit van Amsterdam].

#### **General rights**

It is not permitted to download or to forward/distribute the text or part of it without the consent of the author(s) and/or copyright holder(s), other than for strictly personal, individual use, unless the work is under an open content license (like Creative Commons).

#### **Disclaimer/Complaints regulations**

If you believe that digital publication of certain material infringes any of your rights or (privacy) interests, please let the Library know, stating your reasons. In case of a legitimate complaint, the Library will make the material inaccessible and/or remove it from the website. Please Ask the Library: <https://uba.uva.nl/en/contact>, or a letter to: Library of the University of Amsterdam, Secretariat, Singel 425, 1012 WP Amsterdam, The Netherlands. You will be contacted as soon as possible.

**Chapter 8: Prolonged running increases neurogenesis but fails to increase BDNF or alter neuropathology in the 3xTg mouse model of Alzheimer's disease**

Michael W. Marlatt, Michelle Potter, Thomas A. Bayer, Paul J. Lucassen, Henriette van Praag

*Submitted*

**Abstract**

Reductions in adult neurogenesis have been previously documented in the 3xTg mouse model of Alzheimer's disease, notably occurring at the same age when spatial memory deficits first appeared. As these findings associated reduced neurogenesis with behavioral deficits in the 3xTg model, we tested whether activity and pharmacological interventions known to increase neurogenesis could prevent deficits in spatial memory in the 3xTg model. We chronically administered the antidepressant fluoxetine to one group of mice, allowed open access to a running wheel in another, and combined both treatments in a third cohort. All treatments lasted 11 months in order to test the ability to induce neurogenesis and preserve spatial memory. Backcrossed 3xTg mice had low levels of neurogenesis that were increased by wheel running. However, 3xTg mice, at an age of 20 months, did not exhibit any deficit in spatial learning or memory as measured in the Morris Water Maze. The 3xTg mice expressed prominent intraneuronal A $\beta$  levels in the cortex and amygdala, but very little in the CA1 hippocampal subfield. Running appeared to increase A $\beta$ , while fluoxetine seemed to reduce A $\beta$  accumulations however the overall density of A $\beta$  and AT8 tau accumulations was not significantly altered by the test conditions. Our results indicate that the 3xTg mice, when backcrossed to a C57Bl6 strain, lose their behavioral phenotype documented in the unmodified 3xTg mouse maintained on a hybrid genetic background. We conclude that running and synergistic treatment of running and fluoxetine increases long-term survival of neurons generated during middle-age in the backcrossed 3xTg mouse model of AD.

## **Introduction**

Previous chapters of this thesis established epidemiological, biochemical, and therapeutic reasons to study Alzheimer disease (AD). Modeling AD is frequently performed with transgenic mice carrying multiple mutated copies of the genes known to, at least partially, underlie the disease (see Chapter 8). The popular 3xTg mouse model was first described in 2003 and displays both amyloid beta ( $A\beta$ ) and tau accumulations; these mice are an attractive model to study AD in view of their reported behavioral and neuropathological phenotype that recapitulates several aspects of the disorder (1,2). Initial findings from these mice demonstrated that intraneuronal  $A\beta$  accumulations preceded tau pathology(3). Behavioral deficits could be observed during an early phase of pathology when increasing levels of intraneuronal  $A\beta$  disrupted neuronal integrity and induced cognitive deficits in the mice in the Morris Water Maze (3). The authors further showed that vaccination with an anti- $A\beta$  antibody reversed behavioral deficits by clearing  $A\beta$  deposits, but not tau neuropathology (3).

Adult neurogenesis is regarded as a special type of brain plasticity that influences vulnerability to accumulating deleterious events (4) and may reflect susceptibility to disease. Surprisingly, neurogenesis was never quantified during interventional studies in 3xTg mice. Sex and age-dependent deficits in adult neurogenesis were first described in the 3xTg mice in 2008. Female 3xTg mice were shown to have reduced neurogenesis in the dorsal hippocampus starting at 4 months-of-age and a significant correlation between intraneuronal  $A\beta$  and reduced neurogenesis at 12 months-of age (5). This suggested that deficits in neurogenesis preceded later AD pathology and correlated with behavioral deficits in the animals. This study was instrumental in stimulating interest in neurogenesis as a therapeutic target to reverse behavioral deficits associated with AD.

While aging and disease reduce neurogenesis in adult rodents, neurogenesis is inducible through activity and pharmacology-dependent mechanisms (see Chapters 1, 6, 7). Acute running conditions can reverse the decline in hippocampal neurogenesis and improve spatial memory in aged animals; running increases neurogenesis and improves recall to the location of a submerged platform similar to levels observed in young animals (6). Fewer studies have tested methods of increasing neurogenesis over longer time scales and addressed implications for learning and memory late in life. This is

particularly important in the context of Alzheimer disease, where aging and disease occur simultaneous.

We know that promoter/ transgene constructs can have direct effect on neurogenesis reported in AD mouse models (as reviewed in Chapter 7). Previous work establish that wheel running increased adult neurogenesis in transgenic Amyloid precursor protein (APP) mice with transgenes expressed under the same promoter as used in the 3xTG mice (7), suggesting activity will similarly induce neurogenesis in 3xTg mice. If deficiencies in neurogenesis are responsible for behavioral deficits in the 3xTg mouse, interventions such as running and antidepressant therapy would be able to reverse these deficits. In view of our results in aging wildtype mice (chapter 6) and for reasons discussed earlier (Chapters 5&6), we sought to evaluate the effects of prolonged interventions (11 months) starting in middle age mice (9 months-of age). Such a design bares considerable relevance for prevention and possibly treating humans, where AD is often not discovered until late in the course of the disease when behavioral and neuropathological deficits have manifested already.

While running is a potent stimulus for hippocampal neurogenesis and spatial memory in various mouse strains (8-10), the underlying mechanisms involve a number of effects, such as increasing brain derived neurotrophic factor (BDNF) and angiogenesis (11,12). Running wheel activity stimulates neurogenesis through both effects on stem cell proliferation and on survival of new neurons (13). The antidepressant fluoxetine has been shown to increase neuronal maturation(14). Furthermore, as additive effects of running and fluoxetine treatment had previously potentiated the expression of BDNF mRNA in the brain, we expected that in our present study, synergistic application of running and SSRI treatment would have an aggregate effect greater than either treatment alone (15). As we set out to correlate behavioral changes with the survival of new neurons, here we only measured the survival and phenotype of new cells. Two cohorts of animals were used to evaluate BrdU cell survival at 1 and 11 months of treatment.

We further evaluated the ability of both interventions to impact the extent of neuropathology by measuring A $\beta$  and tau pathology in these animals. A relatively novel aspect of the biochemistry and neuropathology of A $\beta$  is the accumulation of intraneuronal A $\beta$  as observed in human brain (16). Neuropathology in the human brain

suggests that intraneuronal A $\beta$  is one of the earliest pathological events in AD (17). As synaptic pathology correlates better with cognitive dysfunction than the accumulation of amyloid plaques (18), many studies of A $\beta$  seek to establish a mechanistic link between A $\beta$  and the physical damage to synapses and to the eventual neuronal death (19) (reviewed by Gouras)(20). The 3xTg mouse model is unique in that it was the first model to show evidence that intraneuronal A $\beta$  expression could indeed replicate many of the behavioral and complex neuropathological changes present in AD patients (3).

## **Materials and Methods**

### **Mice**

3xTg mice were first generated by Prof. FM LaFerla (University of California, Irvine, USA) and acquired by the National Institute on Aging (NIA, Baltimore, MD, USA). 3xTg mice, harboring PS1M146V, APP<sup>swe</sup>, and tauP301L transgenes, were first backcrossed to the C57Bl6 strain for 7 generations. The mice were maintained on a standard NIH-07 diet (Harlan-Tekland, Indianapolis, IN) with free access to water during a 12-hour light/12-hour dark cycle. Female mice were group housed until the start of the experiment at 9 months-of-age then singly housed for the duration of the experiment. Female 3xTg mice were randomly assigned to control (Con), fluoxetine (Flu), running (Run), and synergistic treatment with fluoxetine and running (FluxRun). Running mice (Run and FluxRun groups) were housed in running wheel cages where running distance was recorded hourly (Clocklab, Coulbourn Instruments, Whitehall, PA).

Two cohorts of animals were used to evaluate acute and chronic responses to the described conditions. Cohort 1: Animals were chronically treated with the conditions listed above for ten months with behavioral testing at 1-month and 10-month time points. Mice were euthanized on day 333, 11 months after the start of the study at 20 months of age. Cohort 2: Animals were treated acutely for 1-month (n= 3-4 per group), to determine the acute effects of treatment on the survival of new neurons labeled in the DG. At the end of each study, animals were deeply anesthetized by isoflurane inhalation and perfused with phosphate buffered saline. Animals were decapitated and brains were immediately removed. The right hemisphere was placed in 4% paraformaldehyde for 48 hrs, followed by equilibration in 30% sucrose.

Tissue was sectioned coronally (40  $\mu\text{m}$ ) on a freezing microtome (Thermo-Fisher) and stored at  $-20^{\circ}\text{C}$  in cryoprotectant solution. The left hemisphere was dissected and frozen on dry ice for biochemical analysis of BDNF. All animal procedures were done in accordance and were approved by the National Institute of Health Animal Care and Use Committee.

### **Administration of fluoxetine in drinking water and running**

Fluoxetine was dissolved in drinking water and replaced every 3 days. A pilot study established that running mice drink comparable amounts of water as sedentary controls. Fluoxetine is soluble in water up to a concentration of 4 mg/ml; in this study we dissolved fluoxetine at 0.12 mg/ml such that oral dosing was 18 mg/kg/day (based on pilot data on water consumption).

Similarly, running animals did not show higher consumption of water compared to sedentary controls. Data from Run and FluxRun groups were recorded and analyzed with Clocklab software: Run  $2.2 \pm 0.6$  km/day, FluxRun  $1.1 \pm 0.5$  km (see Table 1). Data collected from Run and FluxRun mice was highly variable as discussed in the Results.

### **Behavior: Morris Water Maze**

Mice were trained in the Morris water maze(21), to find a platform hidden 5 mm below the surface of a pool (1.40-m diameter) that was filled with water made opaque with white nontoxic paint. Starting points were changed daily for each trial. A trial lasted either until the mouse had found the platform or for a maximum of 60 sec. Mice rested on the platform for 10 sec after each trial. Mice were trained with 4 trials per day over 6 days. Upon completion of training, the platform was removed for 60-sec probe trials; probe trial were held 4 hours and 24 hours after the last training session. Platform latency was recorded (Anymaze, Stoelting Co., USA).

### **Behavior: Rotor-Rod performance**

The Rotor-Rod test was used to assess sensorimotor coordination and motor performance at 10 and 20 months of age. Latency to first fall and the total number of falls were measured during 3 trails of 5 minutes using a program with constant acceleration to 25 rpm.

### **Bromodeoxyuridine immunohistochemistry and cell counts**

In order to analyze newborn cells, BrdU (50 mg/kg) was injected i.p. for the first 10 days for each cohort of animals. A one-in-six series of free-floating sections (40  $\mu$ m) was washed in PBS and pre-incubated with 0.6% H<sub>2</sub>O<sub>2</sub> for 30 minutes. After rinsing, the sections were incubated in 2N HCl at 37° C for 30 minutes to denature DNA then neutralized in 0.1 M Borate buffer at RT. After thorough washing, the sections were blocked with PBS++ (3% Donkey Serum-0.05 M PBS, 0.5% Triton-X 100) for 30 min at room temperature and incubated with rat anti-BrdU (1: 200 in PBS, Accurate Chemical Westbury NY) overnight at 4° C. Thereafter, the sections were washed and immersed in biotin-SP-conjugated donkey anti-rat IgG (1: 250, Jackson ImmunoResearch, West Grove, PA) followed by 2 hrs in ABC reagent (1:800, Vestastain Elite; Vector Laboratories, Burlingame, CA). The sections were then incubated with the substrate 3, 3'-Diaminobenzidine (D4418, Sigma, St. Louis, MO) for 5 min to visualize the cells that had incorporated BrdU. BrdU-positive cells were counted in a one-in-six series of sections (240  $\mu$ m apart) through a 20X objective (Olympus, BX51) throughout 6 hippocampal sections per animal starting at approximately Bregma -1.46.

The volume of the DG for each group of animals was determined by DAPI staining a 1:6 series of sections and outlining the GCL and SGZ on a microscope equipped with Stereoinvestigator software (Microbrightfield). Seven sections were outlined making boundary contour tracings to determine the area of the DG at each level. Area values were used by the Cavalieri method to determine hippocampal volume. No significant differences in total area were found between groups (One-way ANOVA  $p = 0.86$ ,  $F = 0.25$ ).

### **Double immunofluorescence for cell fate analysis**

Free-floating sections (1:6 series) were simultaneously incubated with primary antibodies against BrdU (1: 100 Accurate Chemical Westbury NY) and the neuronal marker NeuN (1:100 Millipore, Billerica, MA) after the denaturation, neutralization, washing and blocking steps described above. Antibodies were diluted in PBS++ and then sections were incubated for 48 hr at 4° C. After rinses with PBS and blocking in PBS++, sections were co-incubated with donkey anti-rat Alexa Fluor 488 (1:250, Molecular Probes, Carlsbad, CA) and donkey anti-mouse Alexa Fluor 568 dyes (1:250, Molecular Probes,

Carlsbad, CA) for 2 hours at room temperature. A laser-scanning microscope was used to identify cells positive for both BrdU and NeuN markers. Fluorescent signals were imaged with a Zeiss LSM 510 confocal laser-scanning microscope and confocal and z-stacked images were used in coordination to determine the percentage of BrdU-positive cells with a neuronal phenotype by expression co-labeling of BrdU with NeuN.

### **A $\beta$ immunohistochemistry and densitometry**

The extent of A $\beta$  immunoreactivity was determined by using a technique documented previously that utilizes formic acid (FA) based antigen retrieval (22). This procedure was modified to accommodate sections cut floating sections cut at 40  $\mu$ m sections. These sections were washed and mounted on Superfrost slides, 4 sections were mounted on each slide. Antigen retrieval was achieved by boiling sections in 0.01 M citrate buffer (pH 6.0) followed by a 3-minute incubation with 88% FA. The primary Ab was directed against N-terminal A $\beta$  peptides (1:250 IBL Japan #18584). Sections were developed using biotinylated secondary Ab, Goat anti-Rabbit 1:200, and Vector Labs ABC (Vector Labs, Burlingame, CA USA). Images, taken at total 100x magnification, were collected on an Olympus BX-51 microscope equipped with a DP-50 camera (Olympus, Hamburg, Germany). Images were converted to 8-bit greyscale images with NIH Image J (v. 1.61) and then converted into binary positive/negative images by using a threshold limit held constant for all images in a given brain region. Percent area fraction was determined through the use of a macro in Image J.

### **Tau immunohistochemistry and densitometry**

As reviewed in Chapters 1 and 7, tau protein is aberrantly hyperphosphorylated at serine and threonine residues during AD. The monoclonal Ab AT8 recognizes tau protein phosphorylated at both serine 202 and threonine 205(23). Tau accumulations can occur in the absence of A $\beta$  and serve as hallmarks for neurodegenerative tauopathies (reviewed by Lee and Goedert) (24,25).

AT8, a mouse monoclonal Ab, is blocked with goat anti-mouse FAb fragments to bind endogenous mouse antigens (1:200 goat anti-mouse FAb fragments diluted in 2% NGS, 0.4% triton, 0.1 M PBS). After subsequent thorough washing (6 x 10 min in PBS), sections were incubated with 1:1000 AT8 for 1 hr at RT and 4°C overnight. The

following day sections were washed and incubated with biotinylated sheep anti-mouse Ab (1:200). Avidin-Biotin complex was applied at the lab-tested concentration (1:800) and sections were developed with diaminobenzene (DAB) according to standard procedures.

### **BDNF Western Blot**

To measure mature BDNF peptide levels, hippocampal tissue was homogenized in 400  $\mu$ l of the 1 X RIPA buffer containing protease inhibitors (Complete Mini, Roche Diagnostics) using pestles and microtubes (ISC BioExpress) and then sonicated with four pulses of 10 seconds at scale 4 (Ultrasonic Processor, Model GE70) at room temperature. The lysed samples were centrifuged at room temperature for 10 min and the supernatants were transferred to fresh tubes. The lysates were reduced with 100 mM DTT at 70°C for 1 h to break the strong disulfide bonds of BDNF. The protein concentrations were measured using Bradford method (Bio-Rad). The samples were diluted to final concentration of 3  $\mu$ g/ $\mu$ l with the lysis buffer and 4 X LDS NuPAGE sample buffer (Invitrogen). Before electrophoresis, the samples were heated at 90°C for 5 min, rapidly cooled on ice for 1 min and then equilibrated to room temperature for 10 min. Equal amounts of 15  $\mu$ g of the proteins were loaded onto 4-12% gradient NuPAGE neutral polyacrylamide gel. The electrophoresis was carried out in 1 X MES buffer and the proteins in the gel were transferred to Immobilon-FL membrane (Millipore) using NuPAGE transfer buffer according to the manufacture's protocol (Invitrogen). The polyclonal rabbit BDNF antibody (Santa Cruz Biotechnology, Inc.) and an infrared-labeled goat against rabbit secondary antibody (Li-Cor Biosciences) were used for immunostaining according to Li-Cor's protocol. The specificity of BDNF antibody staining was confirmed by co-migration with the reduced human recombinant BDNF (0.1  $\mu$ g) monomer (Neuromics).

### **Statistical analysis**

All statistical analyses were carried out using GraphPad Prism. For Morris water maze latency, one way analysis of variance (ANOVA) with repeated measures was performed followed by Bonferroni posthoc tests for individual days. For the time in quadrants, a one-way ANOVA was performed on each group followed by Bonferroni post-hoc

tests. For comparisons of 2 groups, Student's t-test was used to determine if means were significantly different and assign statistical significance.

## Results

### Fluoxetine impairs motor coordination and appears to reduce running distance

Our study design allows us to collect data on running distances in the Run and FluxRun cohort non-invasively during the study. We found surprising evidence that a high degree of variability was present for running distance in the middle-aged 3xTg mice (Table 1). Both Run and FluxRun groups showed similarly large ranges for total distance traveled in the running wheel. This was evident when evaluating data from 28 and 333 days. At both time points, FluxRun animals show lower average distances, however these differences are not significant (Student's 2-tailed t-test, 28 days  $p = 0.61$ , 333 days  $p = 0.09$ ). Fluoxetine did not impair motor coordination at 1 month (data not shown), however impairment was evident at 20 months; Flu mice displayed a significantly higher frequency of falls when measured over three trials in the Rotor-rod test (Fig 1A, One-way ANOVA  $p < 0.05$ ).

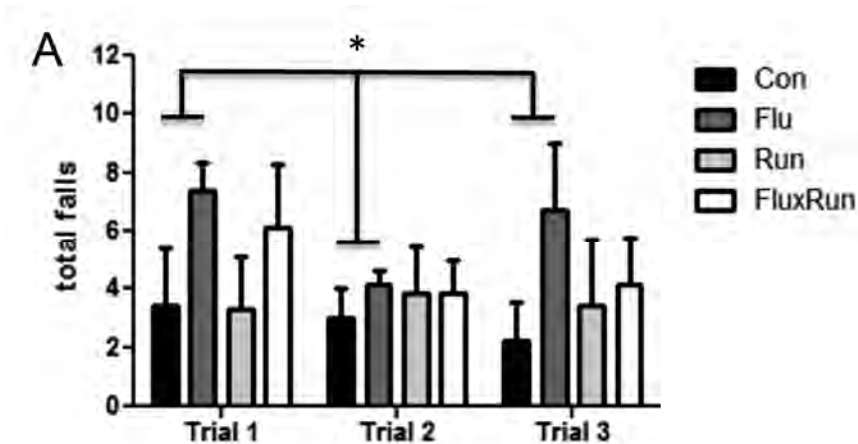


**Fig 1: Total falls in the Rotor-rod test at 20 months of age**

During a program of constant acceleration on the Rotor-rod, 3xTg mice given fluoxetine show a higher total number of falls when measured across trials. All three trials were conducted in succession on the same day with approximately 1 hr between trials (repeated measures ANOVA  $F(3,54) = 5.82$ ,  $p < 0.05$ ).

**Table 1: Total distance range and average for Flu and FluxRun groups**

Data collected from the running wheels reflects that both Run and FluxRun groups has a high degree of variation. FluxRun animals showed a trend for running less distance on average that the Run cohort, however the means are not significantly different (Student's 2-tailed t-test, 28 days  $p=0.61$ , 333 days  $p=0.09$ ).

Group	Days	Range: Total distance (km)	Average distance (km)	Stdev. (km)
Run	1-28	5.4 – 123.0	54.2	51.4
FluxRun	1-28	2.1 – 120.4	40.3	44.3
Run	1-333	231 – 1367	738	461
FluxRun	1-333	28 – 1188	367	420

### **Chronic running stimulates BrdU+ cell survival and adult neurogenesis**

The thymidine analog BrdU was injected for the first 10 days to label dividing neural progenitor cells. To measure the short-term effects of running and fluoxetine, a separate cohort of animals was used to quantify BrdU+ cell survival 1 month after injection when 3xTg mice were 10 months of age. BrdU labeled cells were counted in the SGZ and granule cell layer. At this time there was a high amount of variability between groups and mean cell survival was not significantly different between groups (Fig 2A).

To measure long-term effects of running, fluoxetine and synergistic treatment, BrdU+ cell survival was also measured after 10 months of treatment when the animals were 19 months of age. A significant difference was found between treatment groups, specifically that running and combined treatment had elevated the number of surviving BrdU+ cells (Fig 2B). However, neither group showed a significant correlation between running distances and BrdU+ survival (data not shown: groups combined, Pearson  $r=0.23$ ,  $p=0.2125$ ; Run only, Pearson  $r=0.14$ ,  $p=0.38$ ; FluxRun, Pearson  $r=0.28$ ,  $p=0.27$ ).

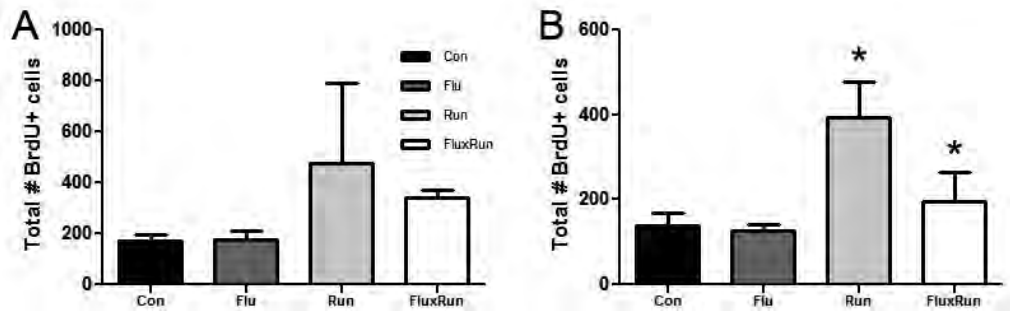


**Fig 2: BrdU+ cell survival 1 month and 11 months after beginning treatment.** A) 1 month after increasing neurogenesis with fluoxetine (Flu), running (Run), or combined therapy (FluxRun), none of the treatment groups show significant elevations in BrdU+ cell survival compared to controls (Con) (One-way ANOVA  $F(3, 9) = 0.97, p = 0.44$ ).

B) 11 months after starting treatment, significant increases in BrdU+ cell survival were seen for both Run and FluxRun groups compared to non-running controls. (One-way ANOVA  $F(3, 23) = 5.27, p < 0.01$ )

### Neuronal differentiation is unaffected by treatments

To investigate the ability of running, fluoxetine, and synergistic treatment to influence adult born cell fate and neurogenesis, confocal imaging was used to identify BrdU+/NeuN+ cells. BrdU in this paradigm identifies cells born during the first 10 days of the experiment while NeuN identifies mature neurons. Co-imaging these markers and quantifying BrdU+/NeuN+ cells across cohorts showed there was no significant difference in the percentage of cells labeled with both markers (control:  $65 \pm 11\%$ , Flu  $59 \pm 7\%$ , Run:  $77 \pm 7\%$ , and FluxRun  $48 \pm 12\%$ )

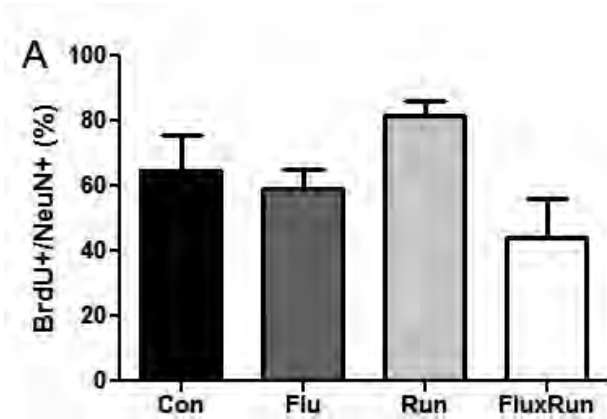


**Fig 3: Percentage of BrdU+ cells expressing the neuronal marker NeuN**

None of the treatment groups showed significant differences in the percentage of BrdU+ newborn cells expressing NeuN as marker for mature CNS neurons (One-way ANOVA  $F(3,19) = 2.27$ ,  $p = 0.11$ )

### **Aged 3xTg mice do not exhibit impairments in learning or memory**

To assess spatial learning and memory, mice were tested in the Morris water maze. Surprisingly, there were no observable differences between groups after 1 month of treatment (Fig. 4A). All animals in the study learned the task to criterion within 6 days, with both groups remembering equally well the location of the platform in a probe test 24 hrs after the last training session. After 11 months of running, at 20 months of age, mice were trained to a different platform location. There was no difference between groups in acquisition of the task over 6 days of training or in the probe tests.

During the 6- and 24-hour probe tasks, mice in Con, Run, and FluxRun had a preference for the target quadrant (Fig 4C, D). Mice treated with fluoxetine, did not show this preference. No differences in swim speed or path length were detected between groups (data not shown).

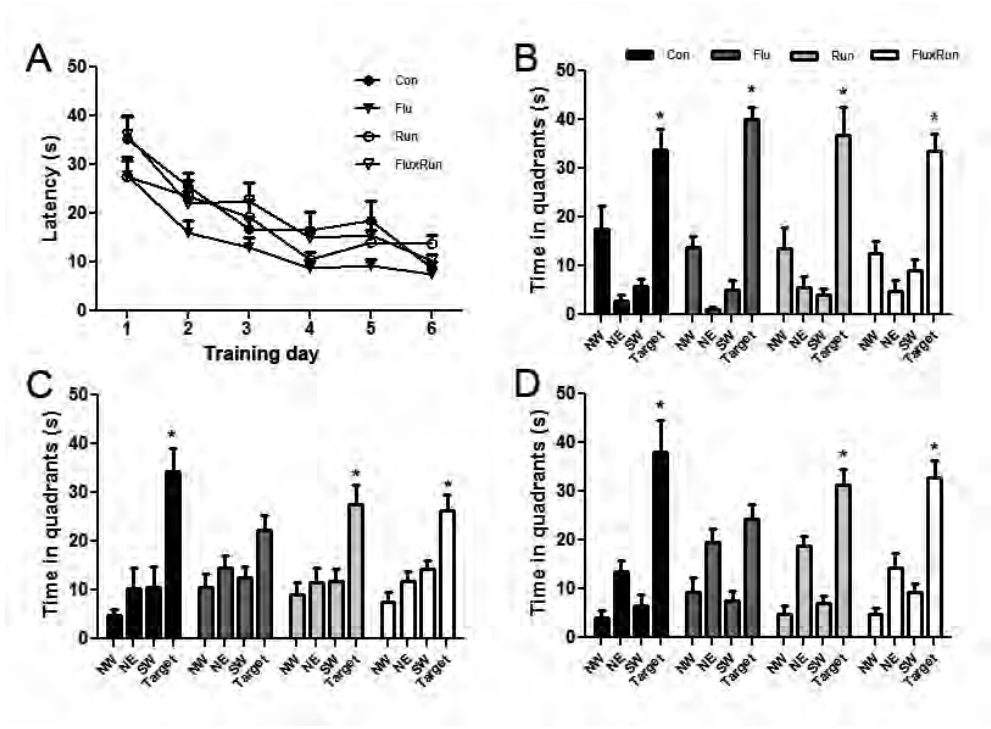


**Fig 4: 3xTg mice show no impairment in learning or memory during testing in the MWM at 10 or 20 months of age.**

A) 1 month data reflects that all groups learned the MWM to criterion (latency to platform < 20s) (repeated measures ANOVA  $F(3,198)= 1.97, p=0.16$ ) and B) remembered the location of the platform 24 hrs after their last training session (Con  $F(3,27)=13.44$ , Flu  $F(3,27)= 54.91$ , Run  $F(3,24)= 11.60$ , FluxRun  $F(3,27)= 17.09$ ,  $P<0.001$ ) Bonferroni post-test  $p<0.05$  target vs each quadrant. . C) 10 months after starting the experiment, 3xTg mice were re-trained and Con, Run, and FluxRun showed significant preferences for the target quadrant during 4 hr probe trials (Con  $F(3,12)=9.00$ , Run  $F(3,21)= 6.00$ , FluxRun  $F(3,18)= 9.34$ ,  $P<0.01$ ) Bonferroni post-test  $p<0.05$  target vs each quadrant, Flu  $F(3,21)= 2.94, p = 0.06$ ) D) 24 hr probe trials (Con  $F(3,12)=13.14$ , Run  $F(3,21)= 21.50$ , FluxRun  $F(3,18)= 22.81$ ,  $P<0.01$ ) Bonferroni post-test  $p<0.05$  target vs each quadrant, Flu  $F(3,21)= 6.61, p <0.01$ ).

### Mature BDNF protein in the hippocampus

Mature BDNF was measured by Western blot; there was no significant difference in BDNF expression between the groups.

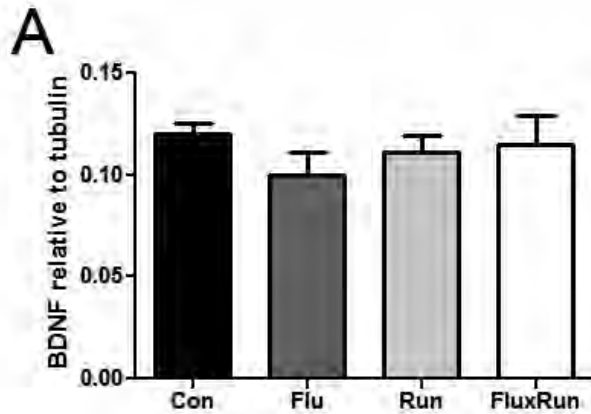


**Figure 5: Mature BDNF protein in the hippocampus**

No significant differences were observed in the amount of soluble BDNF across cohorts. BDNF protein, as measured by Western blot, was standardized to the housekeeping gene, beta-tubulin (One-way ANOVA  $F(3,23) = 0.56$ ,  $p = 0.64$ ).

### A $\beta$ expression in the 3xTg mouse

Markers of AD neuropathology remain a common endpoint to determine the efficacy of a new drug. While fluoxetine has no known pharmacological interaction with any of the enzymes directly related to the generation of A $\beta$  peptide, there are many secondary mechanisms capable of influencing A $\beta$  accumulation of in the brain.

Given the important role of intraneuronal A $\beta$  in the pathogenesis, we used a specific immunocytochemical protocol for intraneuronal A $\beta$ . This technique also identifies extracellular A $\beta$  plaques, but not beta C-terminal fragments ( $\beta$ -CTFs)(supplementary Fig 1). In the rostral hippocampus, intraneuronal A $\beta$  is observable primarily in the cortex and amygdala (Amy) (Fig 6A-B, Fig 7 A-H). In contrast to these areas, extracellular A $\beta$  plaques are predominantly found in the CA1 region and Subiculum (Sub) (Fig 6C-D, Fig 7 I-P). These structures were anatomically identified and quantified across three separate sections that were standardized to specific rostral-

caudal orientation to make appropriate comparisons (representative levels Fig 6). A 1:6 series of tissue sections was used to determine neuropathology, such that neighboring sections are 240  $\mu\text{m}$  apart. If three consecutive sections were not available for quantification within an anatomical region, within the proper rostral-caudal orientation (amygdala and cortex -1.46  $\rightarrow$  -2.30 mm, CA1 -1.94  $\rightarrow$  -2.78 mm, subiculum -2.46  $\rightarrow$  -3.30 mm), the animal was not included for analysis. Missing or damage sections were not frequently observed.

Densitometry was used to measure  $\text{A}\beta$  accumulations, as labeled by immunohistochemistry with anti- $\text{A}\beta$  antibody (IBL #18584) recognizing the N-terminus of  $\text{A}\beta$ . Both intraneuronal and extracellular  $\text{A}\beta$  are recognized by the antibody, similarly densitometry employs a thresholding technique that captures intraneuronal and extracellular  $\text{A}\beta$  information indiscriminately. For each brain subregion, photomicrographs were saved as an image sequence and a threshold was determined that identified specific staining while omitting background staining for the image sequence. The image sequence was then evaluated for percent area fraction using 3 threshold values, namely the originally determined threshold value in addition to one higher and one lower. Under no circumstances did changing the threshold value, used to determine the percent area fraction, change the outcome of the statistical comparison between groups.

This procedure was repeated to evaluate the density of AT8 positive neurons in the caudal CA1. These cells have intense cytoplasmic and basal dendritic staining, including fibers found in the subiculum. A low threshold value was used to selectively identify neuronal cell bodies and minimize the amount of dendritic staining quantified for percent area fraction density measurements.

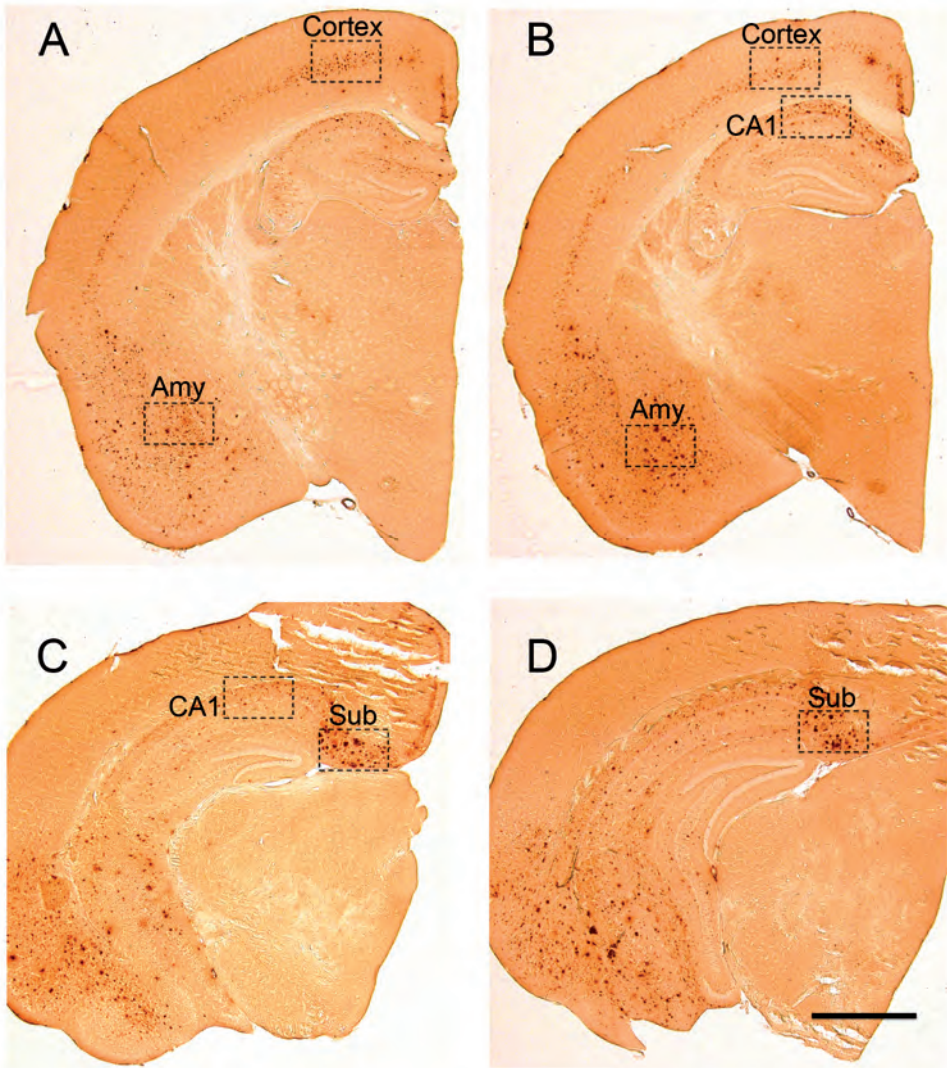


**Figure 6: Overview and regions of interest used for quantification of A $\beta$  pathology in 20 month-old female 3xTg mice.**

A) Cortical and amygdala A $\beta$  pathology were quantified at anatomical levels of approximately Bregma -1.46 mm. B) Cortical, amygdala and CA1 pathology were quantified at -1.94, while quantification of the subiculum continued through -2.46 (C), staining of the subiculum was quantified in the caudal hippocampus, here at -2.70 mm, but as far back as -3.30 mm. scale bar = 600  $\mu$ m.

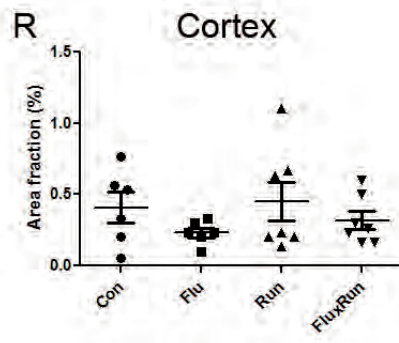
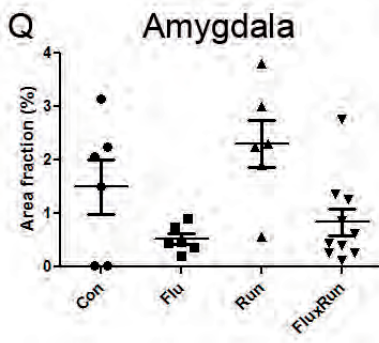
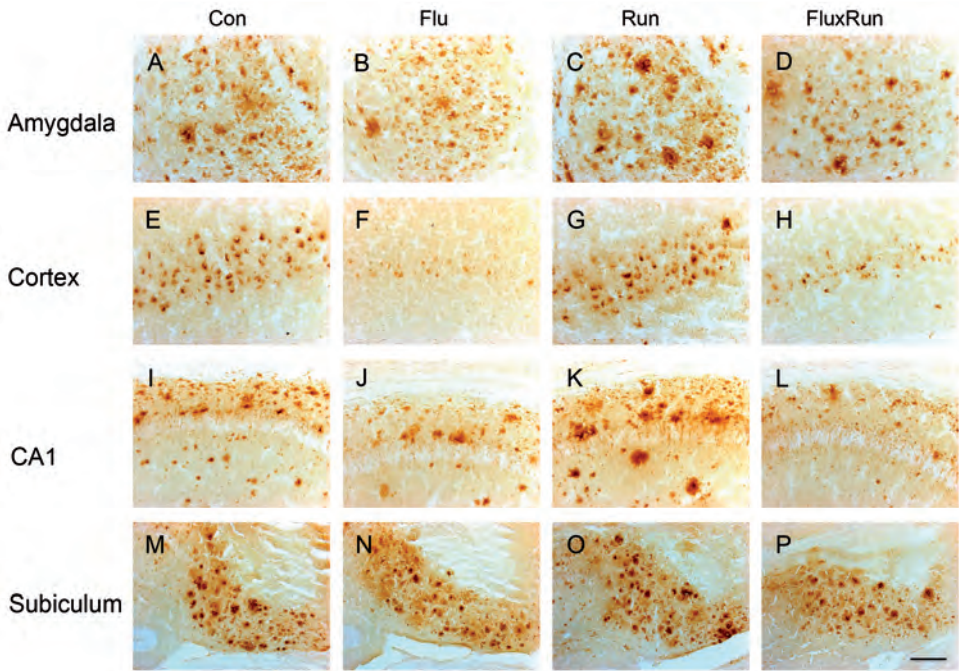


**Figure 7: Intraneuronal A $\beta$  and A $\beta$  plaque load in selected subregions of the 3xTg mouse brain.**

A-D) Examples of A $\beta$  deposition in the amygdala of 3xTg mice, showing intraneuronal A $\beta$  and extracellular A $\beta$  deposits across cohorts. E-H) Intraneuronal A $\beta$  is found in the cortex of all cohorts, however no evidence of extracellular deposits was present. I-J) In the CA1 region, the majority of detected A $\beta$  is present in extracellular plaques, note that no neuronal profiles are seen when compared to the cortex. M-P) Dense staining of extracellular plaques is predominantly found in the subiculum across cohorts (scale bar = 100  $\mu$ m) Q) Densitometry of the amygdala across cohorts reflects that while running appears to increase A $\beta$ , fluoxetine may reduce A $\beta$  accumulations. Flu and FluxRun groups had lower area fraction scores compared to Run, but not to Con. (One-way ANOVA  $F(3,24) = 4.79$ ,  $p < 0.05$ ) Bonferroni post-test Flu vs Run  $p < 0.05$ , FluxRun vs Run  $p < 0.05$ ) R) Similarly, in the cortex fluoxetine appears to reduce A $\beta$  accumulations, however these differences are not statistically significant (One-way ANOVA  $F(3,22) = 1.00$ ,  $p = 0.41$ )

### Hyperphosphorylated tau in the caudal hippocampus

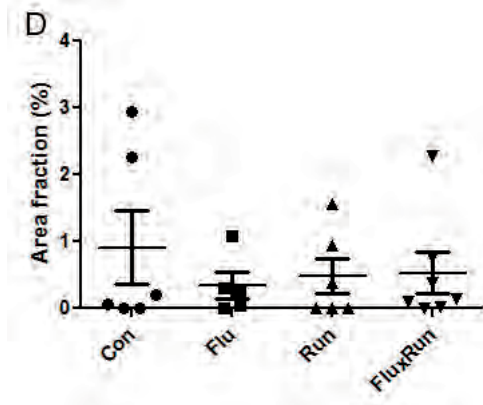
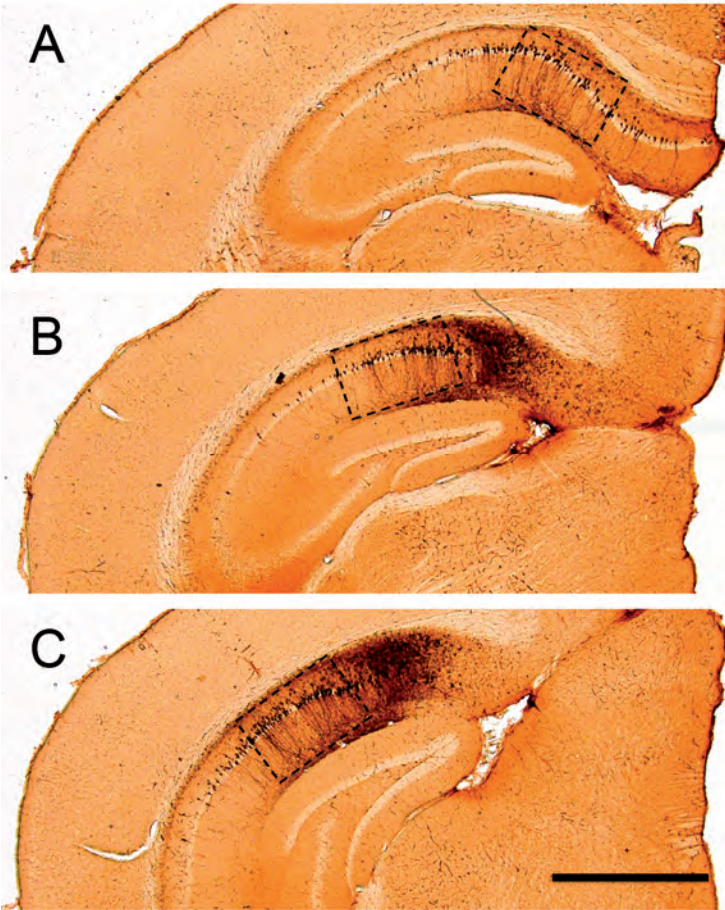


**Figure 8: AT8 tau pathology in the CA1 region of the 3xTg mouse**

A-C) Neurons of the CA1 regions showed robust staining for hyperphosphorylated tau protein as identified by AT8 immunostaining. Sections were rotated while being photographed to exclusively frame the CA1. Quantification was carried out on sections beginning at -1.94 mm Bregma and continuing through approximately -3.16 mm Bregma, scale bar = 600  $\mu\text{m}$ . D) None of the interventions showed an ability to reduce pathological hyperphosphorylation identified by the monoclonal Ab AT8 (ANOVA  $F(3,22) = 0.58$ ,  $p = 0.61$ )

**Discussion**

Our data indicates that running, started in middle-aged 3xTg mice increased neurogenesis in old animals. Cells labeled with BrdU survived in the DG for 11-months indicating that neurons generated in middle-age are maintained through old-age. As we used parallel cohorts to identify cell survival both 1 and 11 months after running and fluoxetine treatment we can see that some loss of the labeled neurons does occur over 10 months (Fig 2 A and B). It appears that only a modest loss of cells occurs during the 10-month interval. Control 3xTg mice had 173 labeled cells (avg) at 10 months-of-age and 149 labeled cells (avg) per DG at 20-months of age. This labeling paradigm is the same as that used in Chapter 6, where control C57Bl6 mice of 15 months of age had 260 labeled cells (avg), suggesting 3xTg mice have lower neurogenesis compared to the C57Bl6 parental strain. This indirect observation suggests backcrossed 3xTg mice have reduced neurogenesis similar to the original report.

In 20 month-old mice, running and synergistic treatment both increased survival of new cells in the dentate. This was observed in fluoxetine treated runners despite evidence that fluoxetine reduces wheel running distance and impairs motor performance. Data collected by the running wheels indicates a trend for reduced total distance in animals given fluoxetine in their drinking water. This agrees with a previous report that fluoxetine can significantly reduce running wheel activity during acute treatment (26). Our evidence suggests that acute fluoxetine treatment is responsible for reduced running wheel activity, but further shows that long-term drug treatment impairs motor coordination in 3xTg mice. This conflicts with other evidence that fluoxetine increases activity in rodents(27,28). Determining if these

effects are dose-dependent, and further exploring acute and chronic effects of fluoxetine may help explain these observations on activity and motor coordination.

Running in the 3xTg mice appeared to be highly variable between animals. This may have contributed to the inability to detect elevated BDNF, as seen in Chapter 6. A previous experiment suggested that synergistic treatment would potentiate BDNF expression; this was done through quantification of BDNF mRNA (15). We did not observe this effect for BDNF protein. Combining this with the observation that neurogenesis was quantitatively lower in the FluxRun group suggests that Fluoxetine and Running cannot be combined in a simple additive manner.

Prior to initiating this experiment, a delayed behavioral phenotype had been observed in the backcrossed 3xTg model at the NIA and we therefore started the experiment later, i.e. when our animals were 9-months of age. Two other experiments demonstrate this delay in phenotype. A study of male 3xTg mice, aged 12-months, reported no behavioral deficits during a 6 week trial of psychosocial stress(29), however a study utilizing male 3xTg mice reported behavioral deficits at 18 months of age (30). All three trials with the backcrossed strain demonstrate a significant delay in phenotype when compared to the original strain where cognitive deficits were documented as early as at 6 months of age in both male and female 3xTg mice (3). Hence, for future research with the 3xTg mice, experiments with the original hybrid strain are preferable. The backcrossed strain appears to have significantly delayed behavioral phenotype that has yet to be systematically reviewed.

The female 3xTg mice in this study showed no deficits in spatial learning or memory during testing in the MWM. Spatial learning and memory measured in the MWM is known to represent learning under stressful conditions; the MWM can produce a robust elevation in corticosterone release in rodents(31). Occupancy of GR receptors is further known to play a critical role in determining performance in the MWM(32). Interestingly, female 3xTg mice show elevated corticosterone levels after 5 days of MWM training, a sexual dimorphism not present in male 3xTg mice (33). Corticosterone levels were not quantified following each trial in our MWM experiments. Future study with the 3xTg model should ideally measure corticosterone concentrations for both sexes. Additional spatial tasks,

such as the Barnes maze, that generally do not induce a stress response, should be used in coordination with the MWM to test the contribution of a stress response to spatial performance.

Other studies have been published regarding wheel running in 3xTg mice. One of the first studies in this area found that wheel running was effective at attenuating sex-specific cognitive deficits in the mice; only the female running mice showed a consistent attenuation of spatial memory problems with exercise (34). Other behavioral changes have been observed, chronic exercise was e.g. shown to prevent deterioration in the anxiety and startle response in the 3xTg mice (35). Outside of the traditional markers of AD neuropathology, wheel running was further shown to reduce markers of oxidative stress in the brains of aged 3xTg mice and to protect mice against an age-related loss of synaptic integrity; the best neuroprotection was attributed to 6 months of running in mice 7 months-of-age(35). A separate study showed that voluntary running increased neurogenesis when evaluated at 9 months of age; running however did not change the fate of the newborn cell phenotypes, which agrees with our results in the same mice (36).

Antidepressants have been under investigation for benefits other than treating depression and anxiety. This includes testing in 3xTg mice for their effects on neurogenesis and neuropathology. Amitriptyline, a tricyclic antidepressant, when given for 4 months was shown to increase neurogenesis, improve performance in the MWM, and increase BDNF protein levels in chronically treated male 3xTg mice (30). Paradoxically however, this study also showed that amitriptyline increased A $\beta$  deposition in the brain. This surprising finding highlights that while antidepressants, such as fluoxetine, without direct pharmacology enzymes responsible for APP cleavage, can nonetheless impact its clearance and deposition. Earlier work had established that paroxetine, another antidepressant from the SSRI class, reduced expression of APP by binding a promoter region in the 5'UTR(37) while additional work with this drug showed cognitive benefits when measured in the Morris Water Maze (38). These studies indicate that antidepressants can exert indirect effects on A $\beta$  plaque deposition in the 3xTg model, each with unique mechanisms of action. Whether these drugs can have a meaningful impact on A $\beta$  deposition in human remains to be determined.

Although the backcrossed 3xTg mice lack a strong behavioral phenotype, the animals used in this experiment were systematically genotyped and exhibited both A $\beta$  and tau accumulations. Determining how backcrossing contributed to behavioral phenotype could be approached experimentally, potentially identifying neuroprotective genes. Identifying gene expression changes between the hybrid and backcrossed 3xTg strain would require additional experiments. Quantitative gene expression changes could be identified by microarray and quantitative PCR for each region of the brain. Identified genes from the screening could be prioritized based on known protein structures and functions. Ideally, western blotting would be utilized in coordination with immunohistochemistry to identify cell-type specific protein expression. Further analysis of soluble and insoluble fractions of A $\beta$  peptide by ELISA might shed light on the proteolytic cleavage of APP. Further experiments would also be needed to identify possible changes in A $\beta$  oligomers and determine if trafficking and/or clearance were altered in the backcrossed strain.

At this time we can only speculate that backcrossing the 3xTg mouse may have led to a loss of intraneuronal A $\beta$  in the CA1. This is difficult to address because we don't have a direct comparison, namely pathology examples from the hybrid 3xTg mouse of the same age produced with the same antibody. In this study we used an antibody directed against N-terminal A $\beta$  (IBL #18584). A similar antibody has been used in the hybrid strain; a monoclonal antibody directed at amino acids 1-5 of N-terminal A $\beta$  (3D6, Elan, South San Francisco, CA, USA) has been used to visualize A $\beta$  deposits have been used in hybrid 3xTg mice at ages of 2, 14, and 20 months, a (39). These authors found that 3D6 labels A $\beta$  deposits across the cortex and pyramidal layer of the CA1 in 2 month-old animals where A $\beta$  appears as perisomatic puncta or granules. The density of these accumulations increases at 14 months, the authors show evidence of 3D6 labeling is fairly prominent in principal neurons at this age. In 20-month-old transgenics puncta are evident in the CA1, where 3D6 labels the neuronal somata, however this is less dense than intraneuronal staining seen in the cortex (39)(Supplemental Fig 2, panels A, B). A conformation specific antibody, which identifies fibrillar oligomers (40), has also been used to identify intraneuronal CA1 staining in hybrid 3xTg mice, aged 18-months, that were maintained on the hybrid background (41) (Supplementary Fig 2 panel E, F). By comparing staining patterns between hybrid and

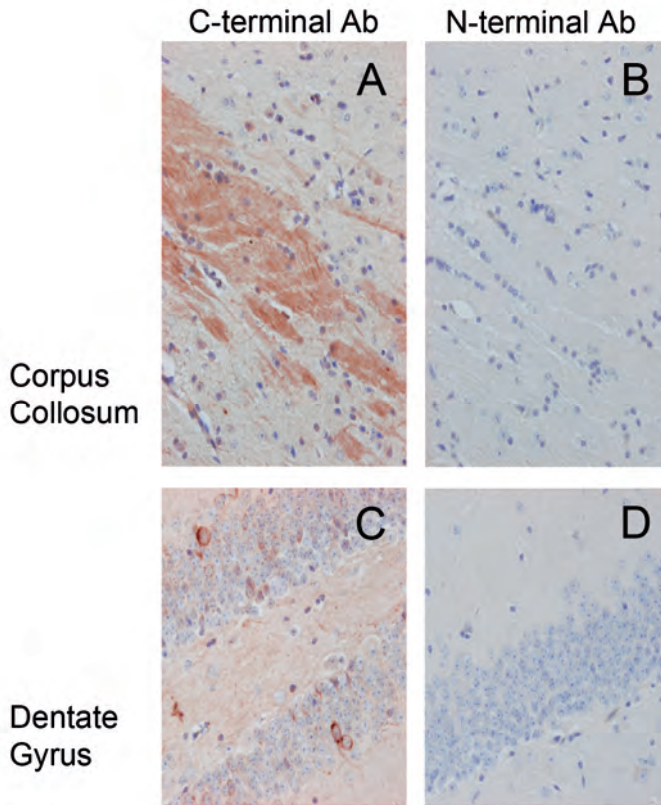
backcrossed 3xTg mice for cortical and hippocampal subregions this limited evidence indicates that a loss of intraneuronal A $\beta$  in the hippocampus may be responsible for the loss of behavioral phenotype.

The study also highlights basic aspects in the generation of mouse models that are worth discussing in detail. Mario Capecchi and Oliver Smithies first described the generation of transgenic mice by somatic recombination of DNA (reviewed by Capecchi)(42) and shared a Nobel Prize with Sir Martin J. Evans for their discovery. Using this technique, DNA is transfected into cells from the Sv129 mouse line, these cells are then microinjected into the blastocyst from the C57Bl6 mouse line (supplemental Fig 3). The animals produced from this procedure are chimeric, expressing regions of Sv129 (with the genetic modification) and C57Bl6 genes. This chimeric mouse must therefore be bred with a mouse from the parental strain, generating an F1 population of animals that are 75% C57Bl6 and 25% Sv129. Subsequent breeding and monitoring transgenic animals allows an investigator to continuously and predictably increase the percentage of the genome derived from the parental strain. This backcrossing approach allows Sv129 genes to be systematically replaced with B57Bl6 genes.

In further discussions of the 3xTg mice, others have observed significant problems with backcrossing and retrieving the originally described phenotype when the mouse embryos are frozen. In personal communications with Dr. Frank LaFerla, he confirmed his lab had done the backcrossing, noticed a significant delay in the onset of the phenotype and immediately stopped working with the backcrossed strain (personal communication). The 3xTg mice are now widely available from commercial vendors, namely the Jackson laboratory. Investigators that have received mice generated from frozen embryo found the phenotype of the animals were significantly delayed (personal communication with Dr. Jorge Palop). For experiments where a reversal of the behavioral deficit is a major study endpoint, the original hybrid 3xTg mouse line is preferable to backcrossed and mice colonies derived from frozen embryos.

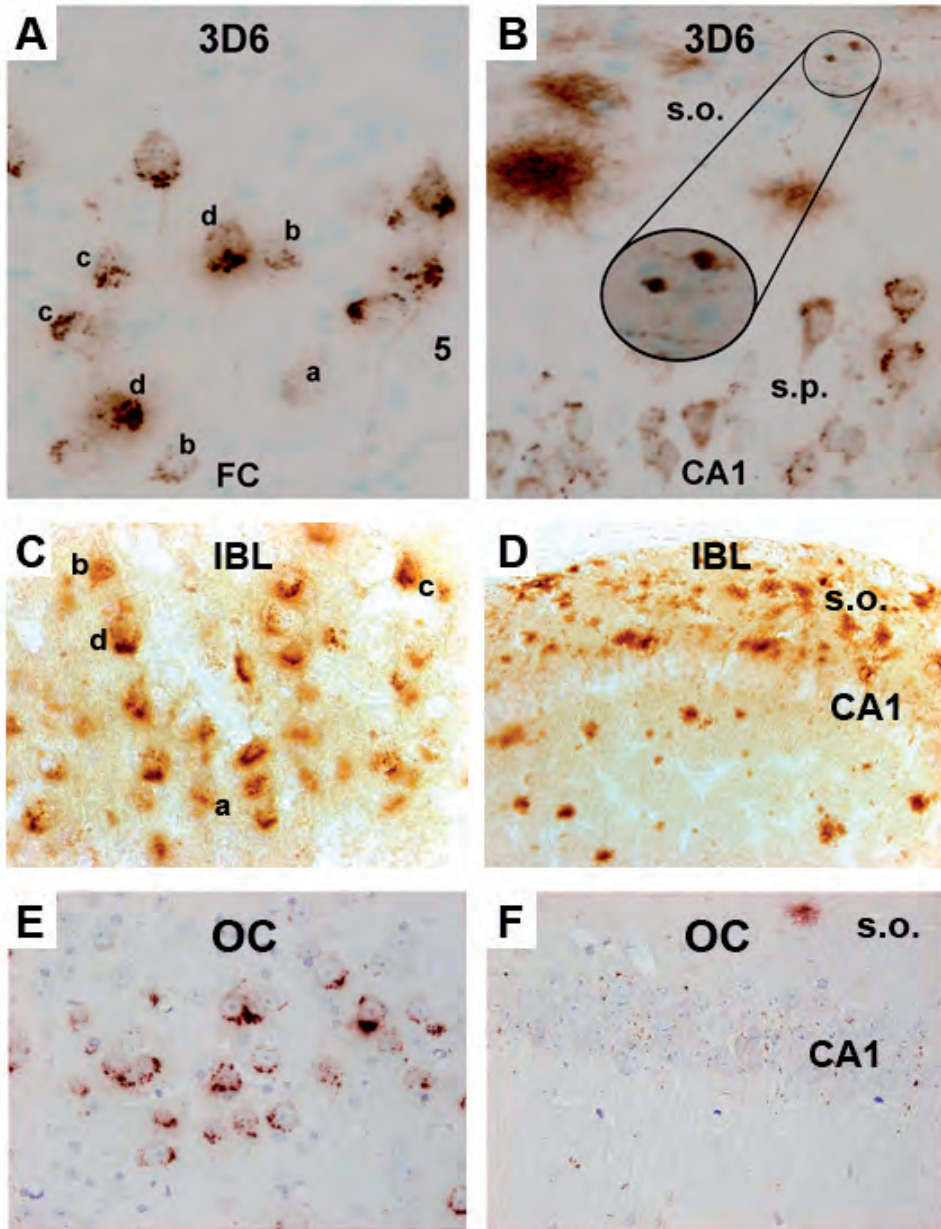
Ultimately, our study shows that neurogenesis is modifiable in 3xTg mice. Behavioral tasks to measure spatial learning and memory, such as the MWM, may not be well adapted or sensitive enough to accurately measure changes in neurogenesis that occur over long time scales. Backcrossing the 3xTg mouse strain should be avoided, as it seems evident that this leads to a significant change in the behavioral

phenotype, thereby diminishing their predictive value as a model of Alzheimer disease.



**Supplementary Fig 1: N-terminal Ab selectively recognizes intraneuronal A $\beta$  and extracellular plaques**

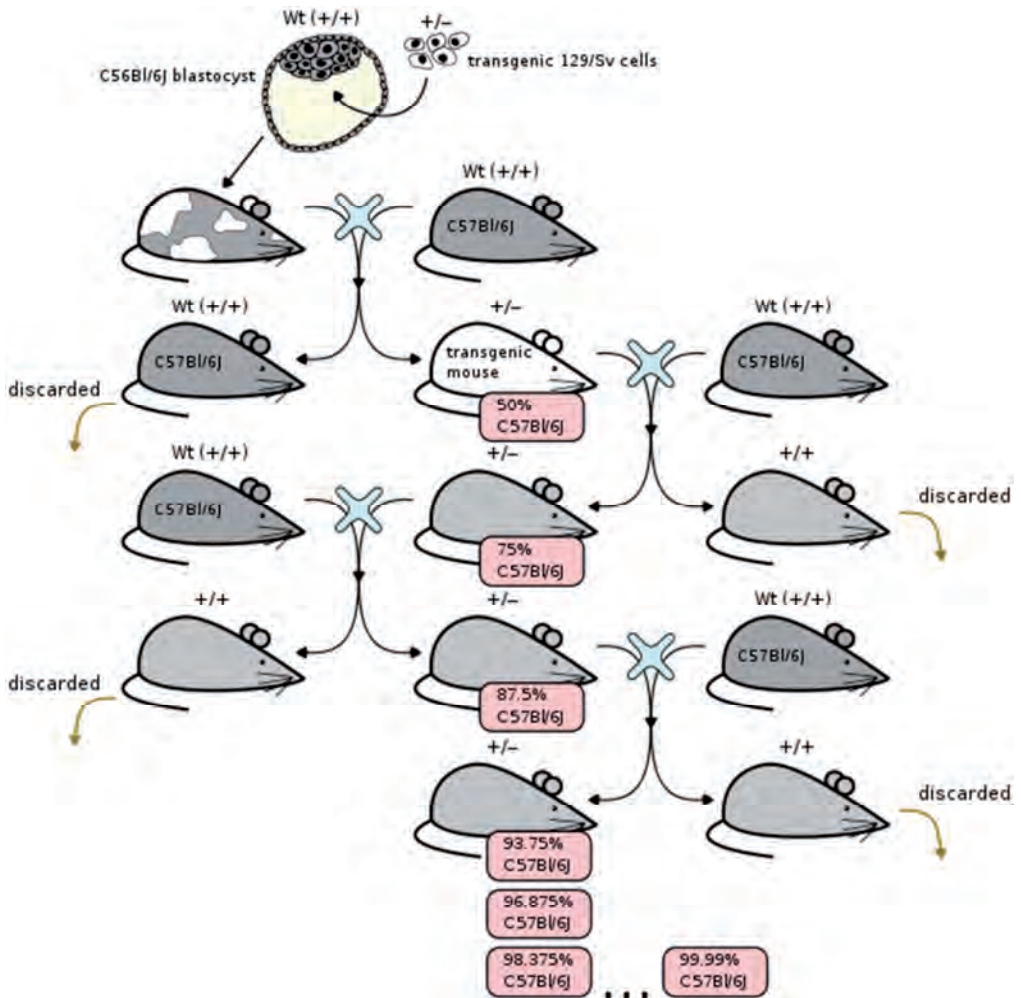
A) Representative staining patterns for the 4 regions examined across the experimental conditions. Intraneuronal A $\beta$  is seen in the amygdala and cortical layers. In the hippocampal CA1 and subiculum, the majority of labeled A $\beta$  is observed in extracellular plaques. B) To rule out the possibility of cross-reactivity of the N-terminal Ab with  $\beta$ -cleaved C terminal fragments (CTFs)(43), SPA4CT mice overexpressing CTFs were immunostained with C-terminal APP Ab (Synaptic Systems, Gottingen, Germany) and the A $\beta$  N-terminal Ab.



**Supplementary figure 2: Comparing cortical and hippocampal A $\beta$  accumulations with 3 antibodies (3D6, IBL, and OC) in aged 3xTg mice**

In an effort to identify differences due to backcrossing, this figure compares cortical and hippocampal staining in 3xTg mice. A) In 20-month-old non-backcrossed mice, intraneuronal A $\beta$  puncta are condensed in the cortex, increasing density of puncta at the axon terminal is denoted by letters a-d B) This is also seen to a lesser extent in the CA1, where 3D6 labels neuronal somata; diffuse plaques, and axonal processes are

also seen in the stratum oriens (s.o.) Panels A, B reproduced from Fig 2 of Cai et al. 2012(39) C) 20-month-old backcrossed mice, presented in this study, show similar intraneuronal puncta in the cortex with identifiable accumulations at the axon terminals D) however no discernable neuronal profiles are seen in the CA1 of backcrossed 3xTg mice indicating that intraneuronal A $\beta$  is absent in these animals E) 18-month old non-backcrossed mice are positive for intraneuronal A $\beta$  as detected by conformation specific OC antibody in the cortex. F) 3xTg mice on the non-backcrossed background show low levels of intraneuronal A $\beta$  in the CA1 when measured with conformation specific OC antibody. Panels E, F adapted from Fig. 4 Wirhth et al. 2011(41).



### Supplemental Figure 3

This diagram shows the rationale for backcrossing a mouse. In this cartoon, the mutation is noted by (+/-), indicating a gene knockout. We see the (+/-) genotype is maintained while the percentage of genes attributed to the C57Bl6J strain increases with each successive crossing (light blue “x”). Genotyping through PCR is needed after each cross to identify the mutant mice. Image credit: [http://en.wikipedia.org/wiki/File:Backcrossing\\_mice\\_from\\_chimera.svg](http://en.wikipedia.org/wiki/File:Backcrossing_mice_from_chimera.svg)

### References

1. Oddo S, Caccamo A, Shepherd JD, Murphy MP, Golde TE, Kaye R, et al. Triple-transgenic model of Alzheimer's disease with plaques and tangles: intracellular Abeta and synaptic dysfunction. *Neuron*. 2003 Jul. 31;39(3):409–421.
2. Oddo S, Caccamo A, Kitazawa M, Tseng BP, LaFerla FM. Amyloid deposition precedes tangle formation in a triple transgenic model of Alzheimer's disease. *Neurobiology of Aging*. 2003 Dec.;24(8):1063–1070.
3. Billings LM, Oddo S, Green KN, McGaugh JL, LaFerla FM. Intraneuronal Abeta causes the onset of early Alzheimer's disease-related cognitive deficits in transgenic mice. *Neuron*. 2005 Mar. 3;45(5):675–688.
4. Kempermann G. The neurogenic reserve hypothesis: what is adult hippocampal neurogenesis good for? *Trends in neurosciences*. 2008 Apr.;31(4):163–169.
5. Rodriguez JJ, Jones VC, Tabuchi M, Allan SM, Knight EM, LaFerla FM, et al. Impaired adult neurogenesis in the dentate gyrus of a triple transgenic mouse model of Alzheimer's disease. *PLoS ONE*. 2008;3(8):e2935.
6. van Praag H, Shubert T, Zhao C, Gage FH. Exercise enhances learning and hippocampal neurogenesis in aged mice. *Journal of Neuroscience*. 2005th ed. 2005 Sep. 21;25(38):8680–8685.
7. Wolf SA, Kronenberg G, Lehmann K, Blankenship A, Overall R, Staufenbiel M, et al. Cognitive and physical activity differently modulate disease progression in the amyloid precursor protein (APP)-23 model of Alzheimer's disease. *Biological psychiatry*. 2006 Dec. 15;60(12):1314–1323.
8. Brown J, Cooper-Kuhn CM, Kempermann G, van Praag H, Winkler J, Gage FH, et al. Enriched environment and physical activity stimulate hippocampal but not olfactory bulb neurogenesis. *The European journal of neuroscience*. 2003 May;17(10):2042–2046.
9. van Praag H, Christie BR, Sejnowski TJ, Gage FH. Running enhances neurogenesis, learning, and long-term potentiation in mice. *Proceedings of the National Academy of Sciences of the United States of America*. 1999 Nov. 9;96(23):13427–13431.
10. van Praag H, Kempermann G, Gage FH. Running increases cell proliferation and neurogenesis in the adult mouse dentate gyrus. *Nature neuroscience*. 1999 Mar.;2(3):266–270.
11. Neeper SA, Gomez-Pinilla F, Choi J, Cotman C. Exercise and brain neurotrophins. *Nature*. 1995 Jan. 12;373(6510):109.
12. Van der Borght K, Kobor-Nyakas DE, Klauke K, Eggen BJ, Nyakas C, Van der Zee EA, et al. Physical exercise leads to rapid adaptations in hippocampal vasculature:

temporal dynamics and relationship to cell proliferation and neurogenesis. *Hippocampus*. 2009 Oct.;19(10):928–936.

13. Kempermann G, Fabel K, Ehninger D, Babu H, Leal-Galicia P, Garthe A, et al. Why and how physical activity promotes experience-induced brain plasticity. *Front Neurosci*. 2010;4:189.

14. Wang JW, David DJ, Monckton JE, Battaglia F, Hen R. Chronic fluoxetine stimulates maturation and synaptic plasticity of adult-born hippocampal granule cells. *Journal of Neuroscience*. 2008th ed. 2008 Feb. 6;28(6):1374–1384.

15. Russo-Neustadt AA, Beard RC, Huang YM, Cotman CW. Physical activity and antidepressant treatment potentiate the expression of specific brain-derived neurotrophic factor transcripts in the rat hippocampus. *Neuroscience*. 2000;101(2):305–312.

16. Gouras GK, Tsai J, Naslund J, Vincent B, Edgar M, Checler F, et al. Intraneuronal Abeta42 accumulation in human brain. *The American Journal of Pathology*. 2000 Jan.;156(1):15–20.

17. Wirths O, Multhaup G, Bayer TA. A modified beta-amyloid hypothesis: intraneuronal accumulation of the beta-amyloid peptide--the first step of a fatal cascade. *J. Neurochem*. 2004 Nov.;91(3):513–520.

18. Terry RD, Masliah E, Salmon DP, Butters N, DeTeresa R, Hill R, et al. Physical basis of cognitive alterations in Alzheimer's disease: synapse loss is the major correlate of cognitive impairment. *Ann. Neurol*. 1991 Oct.;30(4):572–580.

19. Bayer TA, Wirths O. Intracellular accumulation of amyloid-Beta - a predictor for synaptic dysfunction and neuron loss in Alzheimer's disease. *Front Aging Neurosci*. 2010;2:8.

20. Gouras GK, Tampellini D, Takahashi RH, Capetillo-Zarate E. Intraneuronal beta-amyloid accumulation and synapse pathology in Alzheimer's disease. *Acta neuropathologica*. 2010 May;119(5):523–541.

21. Morris R. Developments of a water-maze procedure for studying spatial learning in the rat. *J. Neurosci. Methods*. 1984 May;11(1):47–60.

22. Christensen DZ, Bayer TA, Wirths O. Formic acid is essential for immunohistochemical detection of aggregated intraneuronal Abeta peptides in mouse models of Alzheimer's disease. *Brain Res*. 2009 Dec. 8;1301:116–125.

23. Goedert M, Jakes R, Vanmechelen E. Monoclonal antibody AT8 recognises tau protein phosphorylated at both serine 202 and threonine 205. *Neuroscience letters*. 1995 Apr. 21;189(3):167–169.

24. Lee VM, Goedert M, Trojanowski JQ. Neurodegenerative tauopathies. *Annual review of neuroscience*. 2001;24:1121–1159.

25. Goedert M, Spillantini MG, Cairns NJ, Crowther RA. Tau proteins of Alzheimer paired helical filaments: abnormal phosphorylation of all six brain isoforms. *Neuron*. 1992 Jan.;8(1):159–168.

26. Weber M, Talmon S, Schulze I, Boeddinghaus C, Gross G, Schoemaker H, et al. Running wheel activity is sensitive to acute treatment with selective inhibitors for either serotonin or norepinephrine reuptake. *Psychopharmacology*. 2009 May;203(4):753–762.

27. Brocco M, Dekeyne A, Veiga S, Girardon S, Millan MJ. Induction of hyperlocomotion in mice exposed to a novel environment by inhibition of serotonin

- reuptake. A pharmacological characterization of diverse classes of antidepressant agents. *Pharmacology, biochemistry, and behavior*. 2002 Apr.;71(4):667–680.
28. Prinssen EP, Ballard TM, Kolb Y, Nicolas LB. The effects of serotonin reuptake inhibitors on locomotor activity in gerbils. *Pharmacology, biochemistry, and behavior*. 2006 Sep.;85(1):44–49.
29. Rothman SM, Herdener N, Camandola S, Texel SJ, Mughal MR, Cong WN, et al. 3xTgAD mice exhibit altered behavior and elevated A $\beta$  after chronic mild social stress. *Neurobiology of Aging*. 2011 Aug. 18;:1–12.
30. Chadwick W, Mitchell N, Carroll J, Zhou Y, Park S-S, Wang L, et al. Amitriptyline-mediated cognitive enhancement in aged 3xTg Alzheimer's disease mice is associated with neurogenesis and neurotrophic activity. *PLoS ONE*. 2011;6(6):e21660.
31. Schaaf MJ, Sibug RM, Durland R, Fluttert MF, Oitzl MS, De Kloet ER, et al. Corticosterone effects on BDNF mRNA expression in the rat hippocampus during morris water maze training. *Stress*. 1999 Dec.;3(2):173–183.
32. Oitzl MS, Fluttert M, Sutanto W, De Kloet ER. Continuous blockade of brain glucocorticoid receptors facilitates spatial learning and memory in rats. *The European journal of neuroscience*. 1998 Dec.;10(12):3759–3766.
33. Clinton LK, Billings LM, Green KN, Caccamo A, Ngo J, Oddo S, et al. Age-dependent sexual dimorphism in cognition and stress response in the 3xTg-AD mice. *Neurobiology of disease*. 2007 Oct.;28(1):76–82.
34. Pietropaolo S, Sun Y, Li R, Brana C, Feldon J, Yee BK. The impact of voluntary exercise on mental health in rodents: a neuroplasticity perspective. *Behavioural brain research*. 2008 Sep. 1;192(1):42–60.
35. García-Mesa Y, López-Ramos JC, Giménez-Llort L, Revilla S, Guerra R, Gruart A, et al. Physical exercise protects against Alzheimer's disease in 3xTg-AD mice. *J. Alzheimers Dis*. 2011;24(3):421–454.
36. Rodriguez JJ, Noristani HN, Olabarria M, Fletcher J, Somerville TDD, Yeh CY, et al. Voluntary Running and Environmental Enrichment Restores Impaired Hippocampal Neurogenesis in a Triple Transgenic Mouse Model of Alzheimer's Disease. *Curr Alzheimer Res*. 2011 Apr. 1.
37. Tucker S, Ahl M, Bush A, Westaway D, Huang X, Rogers JT. Pilot study of the reducing effect on amyloidosis in vivo by three FDA pre-approved drugs via the Alzheimer's APP 5' untranslated region. *Curr Alzheimer Res*. 2005 Apr.;2(2):249–254.
38. Nelson RL, Guo Z, Halagappa VM, Pearson M, Gray AJ, Matsuoka Y, et al. Prophylactic treatment with paroxetine ameliorates behavioral deficits and retards the development of amyloid and tau pathologies in 3xTgAD mice. *Exp. Neurol*. 2007 May;205(1):166–176.
39. Cai Y, Zhang X-M, Macklin LN, Cai H, Luo X-G, Oddo S, et al. BACE1 elevation is involved in amyloid plaque development in the triple transgenic model of Alzheimer's disease: differential A $\beta$  antibody labeling of early-onset axon terminal pathology. *Neurotox Res*. 2012 Feb.;21(2):160–174.
40. Kaye R, Head E, Sarsoza F, Saing T, Cotman CW, Necula M, et al. Fibril specific, conformation dependent antibodies recognize a generic epitope common to amyloid fibrils and fibrillar oligomers that is absent in prefibrillar oligomers. *Molecular Neurodegeneration*. 2007;2:18.

41. Wirths O, Dins A, Bayer TA. A $\beta$ PP Accumulation and/or Intraneuronal Amyloid- $\beta$  Accumulation? The 3xTg-AD Mouse Model Revisited. *J. Alzheimers Dis.* 2011 Nov. 21.
42. Capecchi MR. Altering the genome by homologous recombination. *Science.* 1989 Jun. 16;244(4910):1288–1292.
43. Rutten BPF, Wirths O, van de Berg WDJ, Lichtenthaler SF, Vehoff J, Steinbusch HWM, et al. No alterations of hippocampal neuronal number and synaptic bouton number in a transgenic mouse model expressing the beta-cleaved C-terminal APP fragment. *Neurobiology of disease.* 2003 Mar.;12(2):110–120.